JTL 14 (2) 2025
Page: 357-370

Contents list available at Jurnal Teknologi Laboratorium

JURNAL TEKNOLOGI LABORATORIUM

Journal Homepage: www.teknolabjournal.com
ISSN 2580-0191(Online) I ISSN 2338 – 5634(Print)

Original Research

OPEN ACCESS

Micro–macro dissociation of renal injury after short-term graded oral monosodium glutamate exposure in Wistar rats

Muhammad Ali Makaminan [1*], Iyam Manueke [1], Muh Taufiq [1]

[1] Department of Medical Laboratory Technology, Poltekkes Kemenkes Manado, Indonesia

Abstract: Monosodium glutamate (MSG) is commonly used as a flavor enhancer; nevertheless, evidence of early, subclinical kidney damage from short-term oral exposure is scarce. This study assessed dose-dependent proximal tubular damage and its correlation with macroscopic renal observations after graded MSG delivery in rats. Sixteen male Wistar rats were randomly assigned to four groups (n = 4/group): a control group and three groups receiving monosodium glutamate (MSG) at doses of approximately 750, 1500, or 2250 mg/kg/day (MSG750, MSG1500, MSG2250) through oral gavage for a duration of 14 days. Post-necropsy, the kidneys were evaluated macroscopically (kidney weight index, linear dimensions, gross lesions) and histologically. Proximal tubular epithelial cells were enumerated in 20 non-overlapping cortical high-power fields (HPFs) per rat and classified as normal, degenerative, or necrotic; the counts were aggregated to obtain the total number of cells per 20 HPFs. Group disparities were assessed utilizing one-way ANOVA accompanied by Tukey's post-hoc analyses. The macroscopic appearance, kidney weight index, and renal dimensions were consistent between groups (all $p > 0.05$). Conversely, histology revealed a pronounced dose–response relationship: normal tubular cell counts diminished progressively, whereas degenerative and necrotic cell counts increased significantly with escalating MSG doses (overall one-way ANOVA, $p < 0.01$).The highest-dose group demonstrated significant tubular degeneration and necrosis, despite maintaining general morphological integrity. In summary, short-term high-dose oral MSG causes significant, dose-dependent harm to the proximal tubules, which may not be evident upon gross inspection, indicating that the proximal tubule is an early and sensitive target in MSG-related nephrotoxicity.

Keywords: monosodium glutamate; nephrotoxicity; proximal tubular epithelium; quantitative histopathology; Wistar rat.

INTRODUCTION

Monosodium glutamate (MSG) is widely used as a flavour enhancer in processed foods and household cooking, and dietary surveys in China indicate substantial and variable MSG intake across demographic groups and regions [1]. In East and Southeast Asia, observational data suggest that MSG use can modify dietary salt preference and potentially alter overall sodium exposure in young adults [2], which is important in settings where hypertension related to high sodium consumption is already a major public health burden [3,4].

Experimental studies increasingly implicate MSG in renal injury in animal models [5–14]. Repeated MSG administration impairs renal function and induces tubular and interstitial damage, and a range of antioxidant and phytochemical interventions have been shown to attenuate these changes [5–14]. Comparative work in adult and ageing mice shows that MSG and sodium chloride have distinct effects

Corresponding author.
E-mail address: nersali8@gmail.com (Muhammad Ali Makaminan)
DOI: 10.29238/teknolabjournal.v14i2.705
Received 06 November 2025; Received in revised form 20 November 2025; Accepted 30 December 2025

on renal morphology, indicating that MSG-related renal changes cannot be attributed solely to sodium load [13]. Mechanistic studies consistently link MSG toxicity to oxidative stress, inflammation, and dysregulated cell death, with increased oxidative markers, inflammatory mediators, and altered caspase-9 and BCL-2 expression in MSG-exposed kidneys, which can be ameliorated by antioxidant interventions [6–9]. Evidence from liver, brain and skeletal muscle supports converging oxidative and excitotoxic mechanisms involving glutamatergic signalling and mitochondrial dysfunction [3,15–18].

Concurrently, nephrotoxicity research emphasizes early, subclinical detection of kidney damage using sensitive histology and novel biomarkers, because functional and gross anatomical changes often appear late [19–22]. Studies with agents such as cisplatin, colistin, polymyxin B, carbon tetrachloride, thimerosal and other chemotherapeutics show that substantial tubular damage and marked elevations of neutrophil gelatinase-associated lipocalin (NGAL) and kidney injury molecule-1 (KIM-1) can precede overt acute kidney injury and obvious macroscopic abnormalities [20–28]. This work defines a characteristic “micro–macro dissociation”, whereby microscopic tubular injury and biomarker changes are not immediately reflected in gross morphology or traditional functional indices [19–22].

However, several methodological gaps remain when these insights are applied to MSG-induced renal injury. Most MSG animal studies prioritize serum or urinary biochemical indices and renoprotective effects of interventions, while histopathological changes are often described qualitatively or with semi-quantitative scores rather than with a standardized high-power-field-based counting strategy across graded MSG doses [5–13,29]. It remains unclear whether short-term, graded oral MSG exposure produces a clearly ordered pattern of tubular injury that is quantifiable on a per-field basis and whether such microscopic changes occur in the absence of obvious macroscopic renal alterations [5,6,9,10,13]. In addition, the short-term, orally administered dose–response profile of early tubular damage under exposure durations that approximate intensive dietary intake has not been systematically characterized [3,6,13,25], and only a few studies have evaluated gross renal morphology alongside detailed tubular lesions at multiple dose levels, so the extent of micro–macro dissociation in MSG-induced renal injury remains incompletely defined [5,9,10,13]. Taken together, these limitations indicate a lack of systematic evidence on whether short-term, graded oral monosodium glutamate exposure induces a quantitatively ordered pattern of proximal tubular injury that is detectable at the microscopic level but not at the macroscopic level.

In this context, the present study characterizes the dose-dependent effects of short-term oral MSG exposure on renal morphology in Wistar rats by combining macroscopic kidney assessment with standardized high-power-field-based quantification of tubular epithelial cell injury. A 14-day oral dosing regimen was chosen to approximate an intensive, yet realistic pattern of dietary MSG intake in humans rather than extreme chronic exposure [1,2]. We used a harmonized counting protocol based on a fixed number of high-power fields per kidney section and explicit criteria to classify tubular epithelial cells as normal, degenerative, or necrotic, to obtain a sensitive, quantitative description of early tubular injury under graded MSG doses. To our knowledge, no previous MSG nephrotoxicity study has systematically combined short-term graded oral dosing, standardized high-power-field based tubular epithelial cell quantification, and concurrent macroscopic renal assessment to interrogate micro–macro dissociation [5,6,9,10,13]. We hypothesized that repeated oral monosodium glutamate administration for 14 days would produce a dose-ordered increase in proximal tubular degeneration and necrosis without overt macroscopic renal changes, consistent with early subclinical nephrotoxicity. Accordingly, our objectives were to quantify normal, degenerative, and necrotic tubular epithelial cells per defined number of high-power fields in control and MSG-treated groups, to compare these microscopic findings with

macroscopic kidney morphology across dose groups, and to explore the extent of micro–macro dissociation in short-term oral MSG nephrotoxicity.

MATERIAL AND METHOD

Research Design

This randomized controlled animal experiment was conducted from January to June 2022 at the Cytohistotechnology Laboratory, Department of Medical Laboratory Technology, Poltekkes Kemenkes Manado, Indonesia, using predefined gross and microscopic renal endpoints to evaluate renal effects of short-term oral monosodium glutamate (MSG) exposure in rats. The experimental protocol complied with national guidelines for the care and use of laboratory animals and adhered to ARRIVE 2.0 reporting recommendations. All procedures were reviewed and approved by the Health Research Ethics Committee of Manado Health Polytechnic, under approval number DP.04.03/FXXX.28/70/2022.

Population and Samples

The study population comprised healthy male albino Rattus norvegicus aged 10–12 weeks and weighing 200–350 g, obtained from the Minahasa colony breeding facility. Using Federer's formula, a total of 16 rats were allocated to four groups (n = 4 per group): one control group and three MSG dose cohorts. Group allocation was performed by simple randomisation using a random-number list to minimise selection bias. The control group received vehicle only, whereas the treatment groups received MSG at 150 mg/200 g body weight (P1), 300 mg/200 g body weight (P2), or 450 mg/200 g body weight (P3), corresponding to approximately 750, 1500, and 2250 mg/kg/day, respectively. These doses were selected to fall within subacute ranges that have induced renal histological changes without lethality in prior MSG nephrotoxicity models as investigated by Kassab et al., (2021), Koohpeyma et al., (2021) and Celestino et al., (2021). Only clinically healthy animals without signs of overt disease were included in the study.

Materials and Research Tools

MSG of analytical grade was prepared fresh each day in distilled water for oral gavage. Animals were housed in standard polypropylene cages with wood-chip bedding, maintained at 22–25 °C with 50–60% relative humidity on a 12:12 h light–dark cycle, and provided standard laboratory chow and water ad libitum. Equipment included analytical balances, oral gavage probes, a tissue processor, paraffin embedding station, rotary microtome, staining racks, and a light microscope (Olympus CX43) equipped for high-power field (HPF) examination at 400× magnification. Renal tissue was fixed in 10% neutral buffered formalin for at least 24–48 h, processed routinely through graded alcohols and xylene, embedded in paraffin, sectioned at 4–5 µm thickness, and stained with haematoxylin–eosin (H&E) using standard protocols (e.g., 5 min in haematoxylin followed by 2 min in eosin). For microscopic assessment, cortical fields containing proximal tubules were examined at high magnification, and tubular epithelial cells were classified according to pre-specified morphological criteria: normal cells showed intact brush borders, basophilic cytoplasm, and round centrally placed nuclei without vacuolisation; degenerative cells exhibited cytoplasmic vacuolation, cell swelling, and partial brush-border loss with nuclear chromatin clumping but preserved cell outlines; necrotic cells displayed hypereosinophilic cytoplasm, cell shrinkage or lysis, and nuclear pyknosis, karyorrhexis, or karyolysis, including desquamated cells within the tubular lumen.

Collection/Research Stages

After a 7-day acclimatisation period, rats were allocated to the four study groups and received their assigned treatments once daily by oral gavage for 14 consecutive days. The control group received the same volume of distilled water, whereas the MGS-treated groups received MSG solutions corresponding to 150, 300, and 450 mg/200 g body weight (approximately 750, 1500, and 2250 mg/kg/day), respectively. Animals were observed daily for general clinical signs,

behaviour, and food and water intake. At the end of the treatment period, rats were fasted overnight, anaesthetised, and euthanised by an approved method (ketamine–xylazine anaesthesia) followed by exsanguination. Both kidneys were removed through midline laparotomy, gently rinsed in saline, blotted dry, and examined macroscopically for colour, surface texture, capsular integrity, cortical–medullary demarcation, focal lesions, oedema, congestion, mottling, and other visible abnormalities. Kidney weight was recorded to calculate the kidney weight index (g per 100 g body weight), and linear dimensions (length, width, and thickness) were measured using a digital calliper prior to fixation. Representative coronal slices including cortex and outer medulla were then fixed in 10% neutral buffered formalin for at least 24–48 h, processed routinely, and embedded in paraffin. Sections were cut, mounted on glass slides, and stained with H&E as described above. For each animal, 20 non-overlapping HPFs of the renal cortex containing proximal tubules were selected using a systematic uniform random sampling approach: after choosing a random starting field in the outer cortex, subsequent fields were captured in a pre-defined serpentine pattern to avoid field-of-view bias. Histological evaluations were performed by an experienced histopathologist who was blinded to group allocation.

Data Analysis

For each rat, proximal tubular epithelial cells were counted in 20 non-overlapping cortical HPFs and classified as normal, degenerative, or necrotic according to the morphological criteria described above. For each cell category, the counts from all 20 HPFs were then summed to obtain a single animal-level total, expressed as the total number of cells in 20 cortical HPFs per rat (absolute cell counts, not percentages). Group results were reported as mean ± standard deviation (SD) of these animal-level totals and are presented in tables and graphs as “total cells in 20 cortical HPFs per rat”. Cell counting was performed manually using a hand tally counter without image-analysis software. Before inferential analysis, data were checked for normality (Shapiro–Wilk test) and homogeneity of variances (Levene test). When assumptions of normality and homoscedasticity were met, between-group comparisons were performed using one-way analysis of variance (ANOVA) followed by Tukey’s post-hoc test. For ANOVA, F statistics are reported with numerator and denominator degrees of freedom in the format $F(df_1, df_2)$. A two-sided p value < 0.05 was considered statistically significant. Statistical analyses were carried out using standard statistical software (SPSS Version 27.0)

.

RESULTS AND DISCUSSION

Macroscopic Renal Findings

Grossly, kidneys from control and MSG-treated rats appeared similar in size, shape, and external morphology, with smooth surfaces, intact capsules, and clear corticomedullary demarcation in all groups (Figure 1). Macroscopic renal findings are summarized in Table 1. Quantitative assessment showed no statistically significant differences in kidney weight index, renal length, width, or thickness among the control, MSG750, MSG1500, and MSG2250 groups (one-way ANOVA; all $p > 0.05$). Mean kidney weight index values ranged narrowly across groups, and renal dimensions remained comparable irrespective of MSG dose.

Qualitative macroscopic examination revealed no gross abnormalities in any experimental group. Across all animals, kidneys exhibited normal colour, smooth surface texture, intact renal capsules, and clear corticomedullary demarcation. No focal pallor, necrosis, cortical mottling, or evidence of marked congestion or oedema was observed in either control or MSG-treated groups. Subsequent histopathological analysis was therefore performed to evaluate whether microscopic renal alterations were present despite the absence of gross morphological changes.

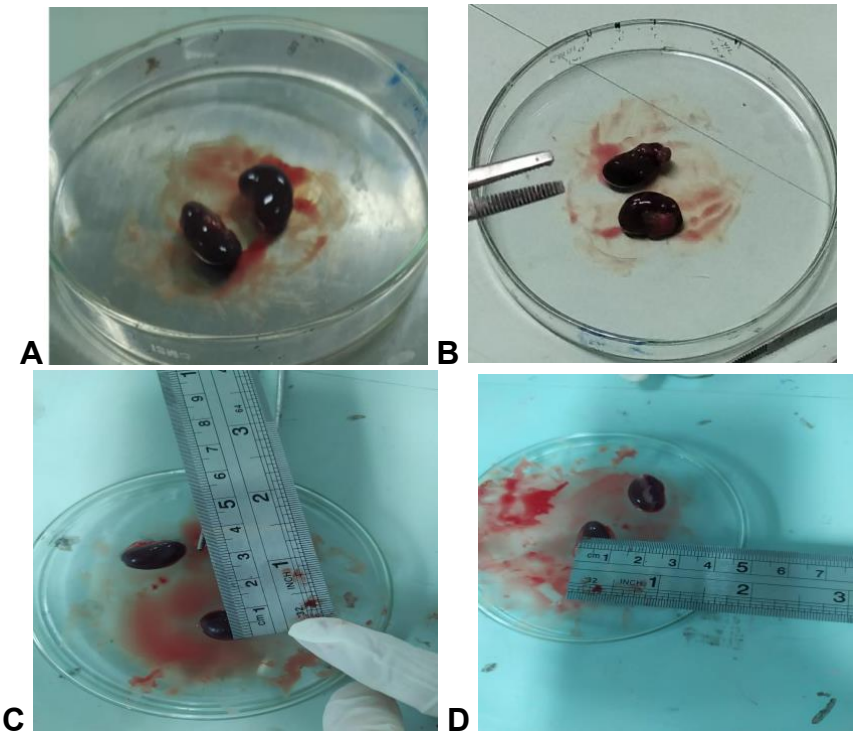

Figure 1. Gross renal morphology of control and monosodium glutamate (MSG)-treated rats following short-term oral exposure.

Representative photographs of kidneys from (A) control rats, (B) MSG750 (≈750 mg/kg/day), (C) MSG1500 (≈1500 mg/kg/day), and (D) MSG2250 (≈2250 mg/kg/day). Across all groups, kidneys appeared comparable in size, shape, surface texture, and external morphology, with intact capsules and no visible gross lesions.

Table 1. Quantitative and Qualitative Macroscopic Renal Findings Across Experimental

Parameter	Control (n = 4)	MSG750 (≈750 mg/kg/day) (n = 4)	MSG1500 (≈1500 mg/kg/day) (n = 4)	MSG2250 (≈2250 mg/kg/day) (n = 4)	p-value*
Quantitative macroscopic parameters					
Kidney weight index (g/100 g BW)	0.80 ± 0.05	0.82 ± 0.06	0.79 ± 0.04	0.81 ± 0.05	0.84
Kidney length (mm)	12.4 ± 0.6	12.6 ± 0.7	12.5 ± 0.5	12.3 ± 0.6	0.92
Kidney width (mm)	7.4 ± 0.3	7.5 ± 0.4	7.3 ± 0.3	7.4 ± 0.4	0.77
Kidney thickness (mm)	5.6 ± 0.3	5.7 ± 0.3	5.5 ± 0.2	5.6 ± 0.3	0.81
Qualitative macroscopic findings					
Abnormal colour	Absent (0/4)	Absent (0/4)	Absent (0/4)	Absent (0/4)	—
Irregular surface texture	Absent (0/4)	Absent (0/4)	Absent (0/4)	Absent (0/4)	—
Capsular adhesion or rupture	Absent (0/4)	Absent (0/4)	Absent (0/4)	Absent (0/4)	—
Blurred corticomedullary demarcation	Absent (0/4)	Absent (0/4)	Absent (0/4)	Absent (0/4)	—
Focal pallor or necrosis	Absent (0/4)	Absent (0/4)	Absent (0/4)	Absent (0/4)	—

Marked congestion or oedema	Absent (0/4)	Absent (0/4)	Absent (0/4)	Absent (0/4)	—
Cortical mottling	Absent (0/4)	Absent (0/4)	Absent (0/4)	Absent (0/4)	—

Note: Values are presented as mean ± SD. *p-values were calculated using one-way ANOVA for quantitative macroscopic parameters only. No statistically significant differences were observed between the control and MSG-treated groups (all $p > 0.05$). Qualitative findings are expressed as presence/absence (number of affected animals/total animals per group).

Although macroscopic renal morphology remained unaltered across all experimental groups, subsequent histopathological analysis revealed dose-dependent microscopic alterations in renal tissue.

Quantitative Tubular Cell Counts

In contrast to the macroscopic observations, quantitative histopathological investigation demonstrated distinct dose-dependent variations in the numbers of proximal tubular epithelial cells. Cell counts for each animal were derived by aggregating category-specific counts across 20 non-overlapping cortical high-power fields (HPFs) per rat (Table 2, Figure 2). The quantity of morphologically normal proximal tubular epithelial cells diminished significantly with escalating MSG dosage. The mean ± standard deviation of normal cell counts per 20 cortical high-power fields decreased from 92.50 ± 7.05 in the control group to 79.75 ± 13.72 in MSG750, 55.25 ± 14.90 in MSG1500, and 11.50 ± 3.10 in MSG2250. One-way ANOVA revealed a highly significant overall group impact for normal cell counts ($F(3,12) = 43.31$, $p < 0.01$). Post-hoc analysis revealed that normal cell counts were considerably diminished in MSG1500 and MSG2250 relative to the control group ($p < 0.01$), but the decrease noted in MSG750 did not achieve statistical significance.

In contrast, the quantity of necrotic proximal tubular epithelial cells significantly escalated with increasing doses of MSG. The mean ± SD necrotic cell counts per 20 cortical high-power fields increased from 12.50 ± 1.29 in the control group to 25.50 ± 4.43 in MSG750, 45.25 ± 4.19 in MSG1500, and 56.00 ± 11.83 in MSG2250. One-way ANOVA demonstrated a significant group effect for necrotic cells ($F(3,12) = 34.05$, $p < 0.01$). Post-hoc analyses revealed that all groups treated with MSG had significantly elevated necrotic cell counts compared to the control group ($p < 0.01$).

Degenerative proximal tubular epithelial cells also exhibited an increase across MSG dosage groups. The mean ± standard deviation of degenerative cell counts per 20 cortical high-power fields were 5.50 ± 1.29 in controls, 20.00 ± 3.82 in MSG750, 26.25 ± 7.27 in MSG1500, and 31.75 ± 5.74 in MSG2250. The group effect was substantial ($F(3,12) = 20.06$, $p < 0.01$). Post-hoc analysis revealed that degenerative cell counts were significantly elevated in all MSG-treated groups relative to controls ($p < 0.01$), although variations within the MSG-treated groups were less evident.

Table 2. Proximal tubular epithelial cell counts in 20 cortical high-power fields (HPFs) per rat in control and MSG-treated groups (n = 4 per group)

Group	**Normal cells** (Mean ± SD)	**Post-hoc p-value vs Control**	**Degenerative cells** (Mean ± SD)	**Post-hoc p-value vs Control**	**Necrotic cells** (Mean ± SD)	**Post-hoc p-value vs Control**
Control	92.50 ± 7.05	–	5.50 ± 1.29	–	12.50 ± 1.29	–
MSG750	79.75 ± 13.72	0.149	20.00 ± 3.82	< 0.01*	25.50 ± 4.43	< 0.01*
MSG1500	55.25 ± 14.90	< 0.01*	26.25 ± 7.27	< 0.01*	45.25 ± 4.19	< 0.01*

MSG2250	11.50 ± 3.10	< 0.01*	31.75 ± 5.74	< 0.01*	56.00 ± 11.83	< 0.01*

Note: Values are expressed as mean ± standard deviation (SD) of animal-level totals. For each rat, proximal tubular epithelial cells were counted in 20 non-overlapping cortical HPFs and classified as normal, degenerative, or necrotic; counts for each category were summed across the 20 fields to obtain total cell counts per rat. One-way ANOVA demonstrated significant group effects for normal ($F(3,12) = 43.31$, $p < 0.01$), degenerative ($F(3,12) = 20.06$, $p < 0.01$), and necrotic cells ($F(3,12) = 34.05$, $p < 0.01$). Pairwise comparisons versus the control group were performed using Tukey's honestly significant difference (HSD) test. *p < 0.01 versus control.

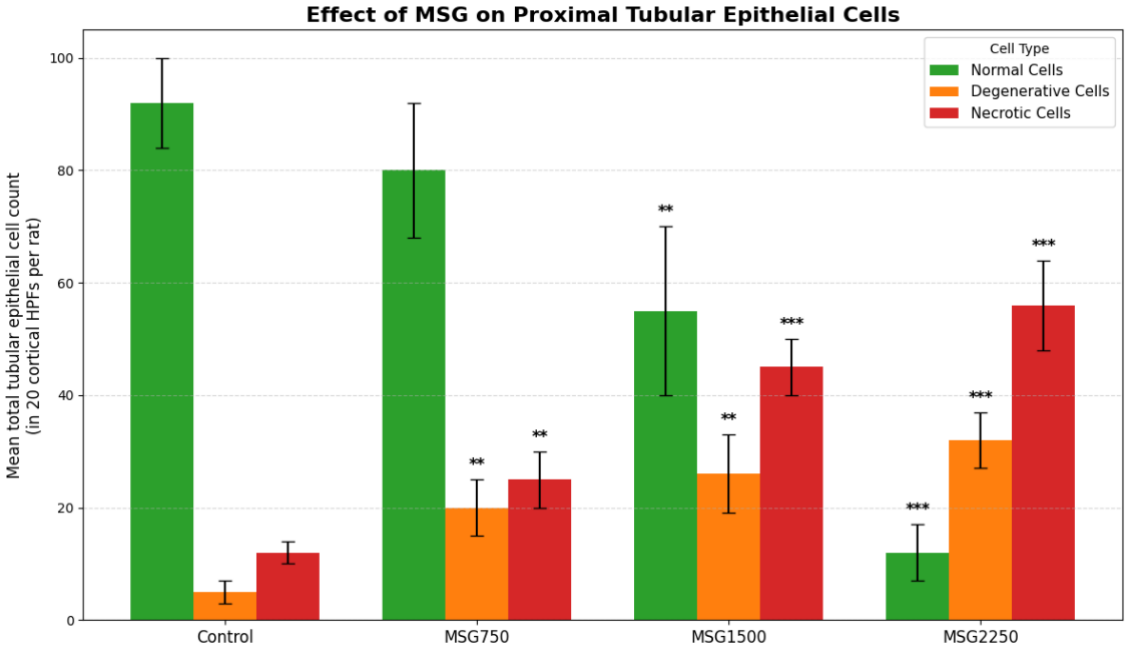

Figure 2. Dose-dependent changes in proximal tubular epithelial cell counts following oral monosodium glutamate exposure.

Bars represent mean ± SD of total proximal tubular epithelial cell counts per 20 cortical high-power fields (HPFs) per rat (n = 4 per group). Green bars indicate normal cells, orange bars indicate degenerative cells, and red bars indicate necrotic cells. Asterisks denote statistically significant differences compared with the control group (* $p < 0.05$, ** $p < 0.01$, *** $p < 0.001$), as determined by one-way ANOVA followed by Tukey's honestly significant difference (HSD) test.

Qualitative Histological Features

Representative H&E-stained sections of the renal cortex are shown in Figure 3. In the control group, proximal tubules displayed normal architecture with intact brush borders, narrow lumina, and tubular epithelial cells with basophilic cytoplasm and centrally located nuclei (black arrows). In MSG750, sporadic degenerative changes were observed, including mild cytoplasmic vacuolation and focal epithelial swelling (yellow arrows), while most tubules retained normal morphology. In MSG1500, degenerative alterations were more frequent and extensive, with tubular epithelial swelling, prominent vacuolation, focal loss of brush border (yellow arrows), and isolated necrotic cells (red arrows). In MSG2250, marked tubular injury was evident, characterised by diffuse epithelial degeneration (yellow arrows), numerous necrotic cells with hypereosinophilic cytoplasm and pyknotic or fragmented nuclei (red arrows), luminal desquamation, and mild tubular dilatation. Interstitial congestion and mild inflammatory cell infiltration were variably present but did not dominate the lesion pattern.

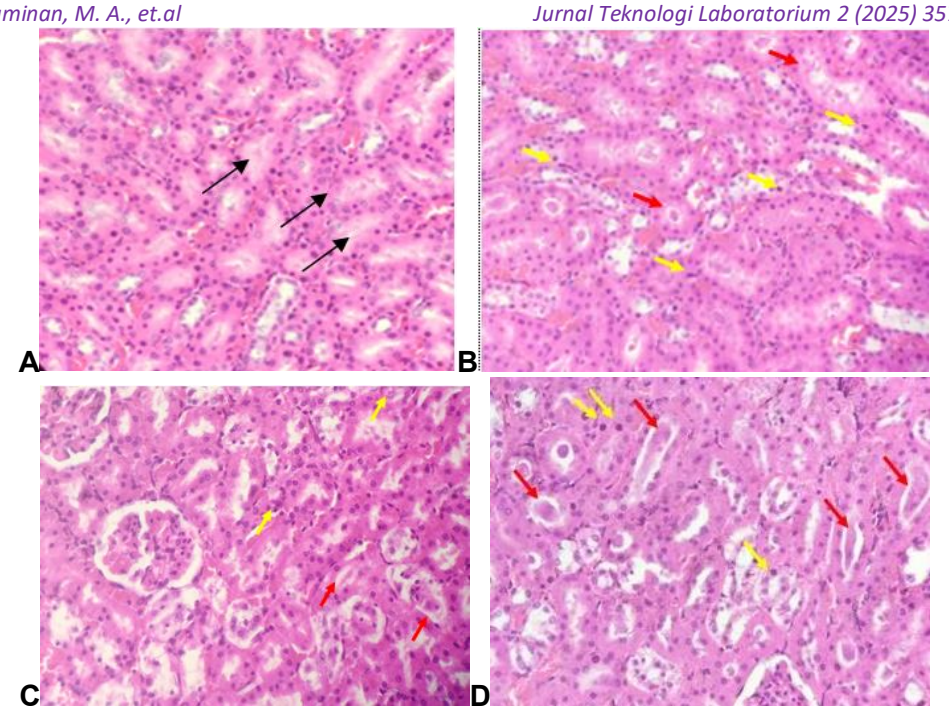

Figure 3. *Representative histopathological features of proximal tubular injury in the renal cortex following graded oral monosodium glutamate exposure.*
Representative H&E-stained sections from (A) control rats showing normal proximal tubules with intact brush borders and centrally located nuclei; (B) MSG750 (≈750 mg/kg/day) showing mild degenerative changes with focal cytoplasmic vacuolation; (C) MSG1500 (≈1500 mg/kg/day) showing more frequent degenerative alterations including tubular swelling, vacuolation, focal brush-border loss, and isolated necrotic cells; and (D) MSG2250 (≈2250 mg/kg/day) showing marked tubular injury with diffuse degeneration, numerous necrotic epithelial cells, luminal desquamation, and mild tubular dilatation. Black arrows indicate morphologically normal proximal tubules; yellow arrows indicate degenerative tubular epithelial cells; red arrows indicate necrotic tubular epithelial cells. H&E staining, original magnification ×400; scale bar = 50 µm.

The present study demonstrates that short-term, graded oral monosodium glutamate exposure is associated with a clear dose-ordered pattern of proximal tubular epithelial injury in Wistar rats, occurring in the absence of detectable gross renal abnormalities. Over the 14-day exposure period, the total number of morphologically normal proximal tubular epithelial cells per 20 cortical high-power fields declined markedly from the control group to the highest-dose group, accompanied by pronounced increases in both degenerative and necrotic cell populations. These quantitative alterations, together with the corresponding qualitative histopathological findings, indicate that the proximal tubular epithelium represents an early and particularly sensitive target of MSG-induced renal injury under the exposure conditions examined.

MSG-related renal injury has been reported in several preclinical models, almost invariably in the context of evaluating antioxidant or phytochemical interventions [5,6,8,11,14,30,31]. Most of these studies describe tubular damage, interstitial oedema, and glomerular alterations and use semi-quantitative histological scores alongside serum creatinine, urea, and oxidative stress indices. Our findings are broadly consistent with their description of MSG-induced nephrotoxicity, but extend this literature by applying a standardised HPF-based counting protocol across three graded oral doses without concomitant renoprotective treatment. By quantifying absolute numbers of normal, degenerative, and necrotic tubular cells per defined area, we demonstrate a clear monotonic dose–response relationship that is more granular than composite histological scores and may be more suitable for future dose–response modelling. To our knowledge, this represents one of the first demonstrations of a quantitatively

ordered, HPF-based dose–response pattern of proximal tubular injury following short-term oral MSG exposure in the absence of renoprotective co-interventions.

Mechanistically, our morphological pattern of vacuolar degeneration, loss of brush border, epithelial swelling, and frank necrosis is compatible with oxidative and inflammatory pathways that have been implicated in MSG toxicity. Studies in which apocynin, protocatechuic acid, honeybee products, curcumin, or plant extracts attenuated MSG-related renal damage consistently report reductions in lipid peroxidation and restoration of antioxidant defences. Studies in which apocynin, protocatechuic acid, honeybee products, curcumin, or plant extracts attenuated MSG-related renal damage consistently report reductions in lipid peroxidation and restoration of antioxidant defences, together with attenuation of tubular injury and inflammatory changes [6,8,11,14,30,31]. Sub-chronic MSG exposure has also been shown to provoke adaptive or defensive responses in renal tissue, including modulation of antioxidant enzymes and stress-responsive pathways in older rats [32], and to alter renal metabolic profiles and gut microbial composition in ways that may enhance oxidative and inflammatory stress [33,34]. Together with reports of hepato-cardiac derangement and systemic metabolic disruption in MSG-treated rodents [32,34,35]. Taken together, these data are consistent with the interpretation that the tubular lesions observed in our study may reflect a broader oxidative and excitotoxic milieu, rather than isolated structural damage, although direct mechanistic measurements were not performed.

Beyond MSG, our observations align with broader nephrotoxicity research showing that proximal tubules are a common and early target for structurally diverse toxicants. Consistent with our observations, a wide range of structurally diverse nephrotoxicants, including antibiotics, chemotherapeutic agents, heavy metals, nanoparticles, and plant-derived toxins, have been shown to preferentially target proximal tubular epithelium, inducing injury mediated by oxidative stress, mitochondrial dysfunction, and tubular cell death [36–42]. In these models, detailed histology and early biochemical markers frequently reveal substantial tubular damage before creatinine rises or kidney size and gross morphology change detectably, reinforcing the concept that highly metabolically active proximal tubules function as a sensitive early warning compartment. Our data suggest that short-term oral MSG exposure can be placed on the same mechanistic continuum, with proximal tubular epithelium again acting as the primary early target.

An important feature of our findings is the pronounced micro–macro dissociation: kidneys remained macroscopically normal in size, colour, and corticomedullary demarcation across all MSG doses, whereas quantitative histopathology documented substantial tubular degeneration and necrosis at the highest dose. This pattern mirrors the disconnect between mild or absent gross changes and extensive microscopic injury reported in other experimental nephrotoxicity settings and mixture risk assessments, where microscopic lesions and biomarker changes emerge long before overt anatomical distortion [36–39,43]. In the context of MSG, such dissociation implies that reliance on gross anatomy or routine functional indices alone may underestimate early kidney injury, particularly under high intake or combined exposure scenarios.

From a translational perspective, the doses used here exceed typical daily MSG intakes reported for most consumers but fall within the range commonly employed in rodent toxicology studies aimed at probing mechanisms and identifying hazard thresholds [5,30,31,33,34]. Our data therefore do not imply that ordinary culinary MSG use will necessarily produce similar tubular damage in humans, but they highlight that repeated high oral doses can elicit marked subclinical tubular injury in the absence of overt macroscopic change. Importantly, these findings should be interpreted within a hazard-identification framework rather than as direct evidence of human risk at typical dietary exposure levels. Given accumulating evidence that MSG can modify renal metabolic profiles, systemic oxidative balance, and gut–renal interactions [32–34], it is plausible that our

histological findings represent one component of a wider risk profile in susceptible individuals, particularly when combined with other nephrotoxicants or cardiometabolic risk factors.

This study has several limitations that should be acknowledged. The sample size in each group was modest, and only male rats were studied, so sex-specific differences in susceptibility could not be explored. The exposure period was relatively short and did not include a recovery phase, precluding conclusions about the persistence or reversibility of MSG-induced tubular injury. We did not measure serum creatinine, blood urea nitrogen, urinary biomarkers, or renal oxidative stress indices in parallel with histopathology, whereas many MSG and non-MSG nephrotoxicity studies have combined biochemical, molecular, and histological endpoints to provide a more integrated picture of injury and protection [6,8,30,31,36,37,39,40]. Ultrastructural changes were not examined by electron microscopy, and we did not undertake detailed quantification of glomerular or interstitial compartments. Finally, manual HPF-based counting is labour intensive and subject to observer variability, although we attempted to minimise bias by using randomised field selection and blinded assessment. Accordingly, the present findings should be viewed as indicative of early histological injury rather than definitive predictors of functional renal impairment.

Future work should therefore combine graded MSG dosing with integrated functional, biochemical, and molecular endpoints, extend exposure and recovery periods, and examine interactions with other dietary or pharmacological nephrotoxicants, potentially using mixture-oriented risk assessment frameworks [36,38,43]. Within such designs, the HPF-based tubular cell counting approach used here could serve as a sensitive histological anchor point for interpreting early biomarker changes. In this context, quantitative HPF-based histopathology may provide a valuable bridge between early molecular perturbations and later functional outcomes. Overall, our findings support the concept that proximal tubular epithelium represents an early and vulnerable target of short-term high-dose oral MSG exposure and underscore the need to consider subclinical histological injury when evaluating renal safety in settings of high MSG intake.

CONCLUSION

In conclusion, short-term graded oral monosodium glutamate administration in Wistar rats is associated with a clear, dose-dependent shift in proximal tubular epithelial morphology, progressing from predominantly normal architecture to marked degeneration and necrosis, while gross renal morphology remains preserved. Quantitative high-power-field–based analysis demonstrated a progressive decline in normal tubular cells accompanied by parallel increases in degenerative and necrotic cells across increasing MSG doses. Together, these findings indicate that proximal tubular epithelium represents an early target of short-term high-dose MSG exposure and that reliance on gross renal morphology alone is insufficient to detect subclinical injury. Although the doses used exceed typical dietary intake and functional biomarkers were not assessed, the pronounced microscopic damage observed in the absence of overt macroscopic change highlights the importance of integrated histological, biochemical, and biomarker-based approaches when evaluating renal safety under conditions of high MSG exposure or combined nephrotoxic stressors.

AUTHORS' CONTRIBUTIONS

Muhammad Ali Makaminan: Conceptualization; Methodology; Resources; Supervision; Project administration. Iyam Manueke: Investigation; Data curation; Formal analysis; Visualization; Writing – original draft. Muh Taufiq: Validation; Writing – review & editing; Methodology; Investigation.

ACKNOWLEDGEMENT

The authors gratefully acknowledge Poltekkes Kemenkes Manado for providing laboratory facilities and logistical support throughout the study. We also thank the laboratory staff and colleagues for their assistance with materials, technical support, and administrative coordination. The authors are solely responsible for the content of this manuscript.

FUNDING INFORMATION

This research received no external funding. All costs associated with the study were covered by the authors' personal funds.

DATA AVAILABILITY STATEMENT

The data supporting the findings of this study are available from the corresponding author upon reasonable request for academic and research purposes.

DISCLOSURE STATEMENT

The views and opinions expressed in this article are solely those of the authors and do not necessarily reflect the official policies or positions of their affiliated institutions. The data presented in this study are original, were generated by the authors, and have not been previously published or submitted for publication elsewhere.

REFERENCE

1. Yu H, Wang R, Zhao Y, et al. Monosodium Glutamate Intake and Risk Assessment in China Nationwide, and a Comparative Analysis Worldwide. *Nutrients*. 2023;15(11):2444. doi:10.3390/nu15112444
2. Morita R, Ohta M, Hayabuchi H. PS-P14-1: Effect Of Monosodium Glutamate On Dietary Salt Reduction In Female Students From East And Southeast Asia: An International Comparison. *Journal of Hypertension*. 2023;41(Suppl 1):e498. doi:10.1097/01.hjh.0000918004.24516.a6
3. Ramadhani A, Sofro ZM, Partadiredja G. The effect of oral administration of monosodium glutamate on orofacial pain response and the estimated number of trigeminal ganglion sensory neurons of male Wistar rats. Gunadi, Yamada T, Pramana AAC, et al., eds. *BIO Web of Conferences*. 2021;41:05007. doi:10.1051/bioconf/20214105007
4. Žakauskienė U, Sukackienė D, Mačionienė E, et al. Ps-P14-2: Arterial Hypertension and Salt Consumption in Lithuania. *Journal of Hypertension*. 2023;41(Suppl 1):e498. doi:10.1097/01.hjh.0000918008.16473.be
5. Farhood zainab H, Eltayef E mahmoud, Madlool ZS. Biochemical Assessment of Hepatic and Renal Functions Following Administration of Doses of Monosodium Glutamate and Shilajit in Albino Mice. Preprint posted online June 20, 2025. doi:10.21203/rs.3.rs-6710430/v1
6. Kassab RB, Theyab A, Al-Ghamdy AO, et al. Protocatechuic Acid Abrogates Oxidative Insults, Inflammation and Apoptosis in Liver and Kidney Associated With Monosodium Glutamate Intoxication in Rats. *Environmental Science and Pollution Research*. 2021;29(8):12208-12221. doi:10.21203/rs.3.rs-731074/v1
7. Koohpeyma F, Siri M, Allahyari S, Mahmoodi M, Saki F, Dastghaib S. The effects of L-carnitine on renal function and gene expression of caspase-9 and Bcl-2 in monosodium glutamate-induced rats. *BMC Nephrology*. 2021;22(1):162. doi:10.1186/s12882-021-02364-4
8. Elmas MA, Özgün G, Özakpınar ÖB, Güleken Z, Arbak S. Effects of Apocynin Against Monosodium Glutamate-Induced Oxidative Damage in Rat Kidne. *European Journal of Biology*. 2022;0(0):0. doi:10.26650/eurjbiol.2022.1148934

9. Abd-Elkareem M, Soliman M, El-Rahman MAMA, Khalil NSA. Effect of Nigella Sativa L. Seed on the Kidney of Monosodium Glutamate Challenged Rats. *Frontiers in Pharmacology*. 2022;13. doi:10.3389/fphar.2022.789988
10. Rahajeng ADR, Rahmatullah AA, Putri CEA, et al. Nephroprotective Effect of Dayak Onion (Eleutherine palmifolia) Against Monosodium Glutamate-Induced Renal Toxicity in Mice (Mus musculus). *Journal of Applied Veterinary Science And Technology*. 2024;5(2):129-134. doi:10.20473/javest.V5.I2.2024.129-134
11. Uroko R, Agbafor A, Egba S, Nwuke C, Kalu-Kalu S. Evaluation of antioxidant activities and haematological effects of Asystasia gangetica leaf extract in monosodium glutamate-treated rats. *Lekovite sirovine*. 2021;41(1):5-11. doi:10.5937/leksir2141005U
12. ALhamed TA, Farah A. Al-marzook, Al-Asady AM. The harmful Effects of Monosodium Glutamate on Blood Parameters Liver and Kidney Functions In Adult White Rats and the Protective Role of Omega-3. *Indian Journal of Forensic Medicine & Toxicology*. 2021;15(3):5245-5250. doi:10.37506/ijfmt.v15i3.16266
13. Celestino M, Balmaceda Valdez V, Brun P, Castagliuolo I, Mucignat-Caretta C. Differential effects of sodium chloride and monosodium glutamate on kidney of adult and aging mice. *Scientific Reports*. 2021;11(1):481. doi:10.1038/s41598-020-80048-z
14. Egbuonu ACC, Alaebo PO, Uchukwu CN, et al. Therapeutic Artemether-Lumefantrine Modulated Monosodium Glutamate-Related Adversity on Rats' Kidney Histology and Antioxidant Response Bio-Indicators. *Journal of Applied Sciences and Environmental Management*. 2021;25(5):807-814. doi:10.4314/jasem.v25i5.18
15. Tosun H, Karadas H, Ceylan H. Bioinformatics-based identification of hepatocellular carcinoma-associated hub genes and assessment of the restorative effect of tannic acid in rat liver exposed to monosodium glutamate. *Cancer Medicine*. 2024;13(12). doi:10.1002/cam4.7404
16. Thangachi SB, Mokhashi VS, Murthuza AA. Analysis Of Oxidative Stress Markers In Chronic Consumption Of Monosodium Glutamate On Liver Of Wistar Albino Rats. *Asian Journal of Pharmaceutical and Clinical Research*. Published online November 7, 2021:116-119. doi:10.22159/ajpcr.2021.v14i11.43103
17. Ibiyeye R, Imam A, Adana M, Sulaimon F, Ajao M. NR2B-DAPK1-P53 mediated hippocampal cell death following monosodium glutamate ingestion and interventions with luteolin, caffeic-acid and phoenix dactylifera. *Nepal Journal of Neuroscience*. 2022;19(3):3-8. doi:10.3126/njn.v19i3.47346
18. Bölükbaş F. Histopathological and Immunohistochemical Study to Determine the Effects of Monosodium Glutamate on Skeletal Muscle Development in Chickens. *Kocatepe Veterinary Journal*. Published online 2023. doi:10.30607/kvj.1223940
19. Liang J, Liu Y. Animal Models of Kidney Disease: Challenges and Perspectives. *Kidney360*. 2023;4(10):1479-1493. doi:10.34067/KID.0000000000000227
20. Dimov N, Yaneva A, Valcheva E, et al. Biomarkers for Early Detection of Cisplatin-Induced Nephrotoxicity. *Life*. 2025;15(9):1432. doi:10.3390/life15091432
21. McMahon KR, Chui H, Rassekh SR, et al. Urine Neutrophil Gelatinase-Associated Lipocalin and Kidney Injury Molecule-1 to Detect Pediatric Cisplatin-Associated Acute Kidney Injury. *Kidney360*. 2022;3(1):37-50. doi:10.34067/KID.0004802021
22. Miloševski-Lomić G, Kotur-Stevuljević J, Paripović D, et al. Integrated Urinary Biomarkers Can Predict Early Acute Kidney Injury in Children Undergoing Chemotherapy. Published online 2023. doi:10.21203/rs.3.rs-3546589/v1

23. Roy D, Kulkarni A, Chaudhary M, Chaudhary S, Payasi A, Aggarwal A. Polymyxin B-Induced Kidney Injury Assessment of a Novel Formulation of Polymyxin B (VRP-034) in Rats. *Antibiotics*. 2021;10(4):359. doi:10.3390/antibiotics10040359
24. Pavitrakar VN, Mody R, Ravindran S. Protective effects of recombinant human golimumab and pentoxifylline in nephrotoxicity induced by cisplatin. *Journal of Biochemical and Molecular Toxicology*. 2022;36(4). doi:10.1002/jbt.22990
25. Kook MS, Kim H, Choi Y, Bae SM, Yu J, Kim YS. The α-Helical Amphipathic Peptide Alleviates Colistin-Induced Nephrotoxicity by Maintaining Mitochondrial Function in Both In Vitro and In Vivo Infection Models. *Antibiotics*. 2025;14(5):445. doi:10.3390/antibiotics14050445
26. Manhar N, Singh SK, Yadav P, et al. Methyl Donor Ameliorates CCl 4 -Induced Nephrotoxicity by Inhibiting Oxidative Stress, Inflammation, and Fibrosis Through the Attenuation of Kidney Injury Molecule 1 and Neutrophil Gelatinase-Associated Lipocalin Expression. *Journal of Biochemical and Molecular Toxicology*. 2025;39(3). doi:10.1002/jbt.70188
27. Ijaz MU, Majeed SA, Asharaf A, et al. Toxicological effects of thimerosal on rat kidney: a histological and biochemical study. *Brazilian Journal of Biology*. 2023;83. doi:10.1590/1519-6984.242942
28. Muğlu H, İnan Kahraman E, Sünger E, Murt A, Bilici A, Görgülü N. Acute Kidney Injury Secondary to Abdominal Compartment Syndrome: Biomarkers, Pressure Variability, and Clinical Outcomes. *Medicina*. 2025;61(3):383. doi:10.3390/medicina61030383
29. Egbuonu ACC, Alaebo PO, Obike CA, et al. Antioxidant and Nephroprotective Studies on Telfairia occidentalis Pod in Experimental Rats. *Nigerian Journal of Biochemistry and Molecular Biology*. 2024;39(2):99-105. doi:10.4314/njbmb.v39i2.9
30. Mahmoud HS, Kamel EM, Gad EL-Hak HN, et al. Potential Ameliorative Effect of Crude Honeybee on Monosodium Glutamate Induced Nephrotoxicity to Male Rats. *The Egyptian Journal of Hospital Medicine*. 2022;89(2):7719-7726. doi:10.21608/ejhm.2022.277126
31. Slima S, Ragab R. Protective Effect of Curcumin Against Monosodium Glutamate-Induced Oxidative Renal Damage: biochemical and histopathological study Received in original form: 23 September 2022 Accepted finally: 5 December 2022. *Ain Shams Journal of Forensic Medicine and Clinical Toxicology*. 2023;40(1):66-73. doi:10.21608/ajfm.2023.281729
32. Moldovan OL, Vari CE, Tero-Vescan A, et al. Potential Defence Mechanisms Triggered by Monosodium Glutamate Sub-Chronic Consumption in Two-Year-Old Wistar Rats. *Nutrients*. 2023;15(20):4436. doi:10.3390/nu15204436
33. Nahok K, Phetcharaburanin J, Li J V, et al. Monosodium Glutamate Induces Changes in Hepatic and Renal Metabolic Profiles and Gut Microbiome of Wistar Rats. *Nutrients*. 2021;13(6):1865. doi:10.3390/nu13061865
34. Sukmak M, Kyaw TS, Nahok K, et al. Urinary metabolic profile and its predictive indexes after MSG consumption in rat. Shakaib M, ed. *PLOS ONE*. 2024;19(9):e0309728. doi:10.1371/journal.pone.0309728
35. Banerjee A, Mukherjee S, Maji BK. Monosodium glutamate causes hepato-cardiac derangement in male rats. *Human & Experimental Toxicology*. 2021;40(12_suppl):S359-S369. doi:10.1177/09603271211049550
36. Balaha MF, Alamer AA, Eisa AA, Aljohani HM. Shikonin Alleviates Gentamicin-Induced Renal Injury in Rats by Targeting Renal Endocytosis, SIRT1/Nrf2/HO-1, TLR-4/NF-κB/MAPK, and PI3K/Akt Cascades. *Antibiotics*. 2023;12(5):826. doi:10.3390/antibiotics12050826
37. Aboelwafa HR, Ramadan RA, Ibraheim SS, Yousef HN. Modulation Effects of Eugenol on Nephrotoxicity Triggered by Silver Nanoparticles in Adult Rats. *Biology*. 2022;11(12):1719. doi:10.3390/biology11121719

38. Sandhiutami NMD, Desmiaty Y, Pitaloka PDU, Salsabila S. The protective effect of hydroalcoholic Citrus aurantifolia peel extract against doxorubicin-induced nephrotoxicity. *Research in Pharmaceutical Sciences*. 2024;19(5):591-605. doi:10.4103/RPS.RPS_99_23
39. Ahmed YH, El-Naggar ME, Rashad MM, M.Youssef A, Galal MK, Bashir DW. Screening for polystyrene nanoparticle toxicity on kidneys of adult male albino rats using histopathological, biochemical, and molecular examination results. *Cell and Tissue Research*. 2022;388(1):149-165. doi:10.1007/s00441-022-03581-5
40. Ryabova Y V, Minigalieva IA, Sutunkova MP, et al. Toxic Kidney Damage in Rats Following Subchronic Intraperitoneal Exposure to Element Oxide Nanoparticles. *Toxics*. 2023;11(9):791. doi:10.3390/toxics11090791
41. Pei Z, Wu M, Yu H, et al. Isoliquiritin Ameliorates Cisplatin-Induced Renal Proximal Tubular Cell Injury by Antagonizing Apoptosis, Oxidative Stress and Inflammation. *Frontiers in Medicine*. 2022;9. doi:10.3389/fmed.2022.873739
42. Upadhyay R, Batuman V. Aristolochic acid I induces proximal tubule injury through ROS/HMGB1/mt DNA mediated activation of TLRs. *Journal of Cellular and Molecular Medicine*. 2022;26(15):4277-4291. doi:10.1111/jcmm.17451
43. Brand A, Bokkers B, Biesebeek JD t., Mengelers M. Combined Exposure to Multiple Mycotoxins: An Example of Using a Tiered Approach in a Mixture Risk Assessment. *Toxins*. 2022;14(5):303. doi:10.3390/toxins14050303